

HOSTED BY



Contents lists available at ScienceDirect

Journal of King Saud University – Science

journal homepage: [www.sciencedirect.com](http://www.sciencedirect.com)

Original article

# The adsorption behavior of individual Cu(II), Zn(II), and Cd(II) ions over a CuO-modified ceramic membrane synthesized from fly ash



Fransisca Widhi Mahatmanti\*, Jumaeri Jumaeri, Ella Kusumastuti

Chemistry Study Program, Faculty of Mathematics and Natural Sciences, Universitas Negeri Semarang, D6 Building 2nd floor, Sekaran Campus, Gunungpati, Semarang, Central Java 50229, Indonesia

## ARTICLE INFO

## Article history:

Received 8 March 2022

Revised 15 August 2023

Accepted 24 August 2023

Available online 28 August 2023

## Keywords:

Ceramic membrane

Fly ash

CuO

Adsorption

## ABSTRACT

The ceramic membrane synthesized from fly ash as the base material with the addition of CuO was used as an adsorbent for Cu(II), Zn(II), and Cd(II) ions in an aqueous solution. The effect of CuO on the characteristics and adsorption activity of fly ash-based ceramic membrane has been studied over Cu(II), Zn(II) and Cd(II) ions with different pH of 2–8, contact time of 30–150 min, and initial concentration of metal ions of 0.1–0.7 mmol/L. The adsorption using the batch method was carried out on Cu(II), Zn(II), and Cd(II) ions individually. This study showed that the surface area and the total pore volume of the fly ash-based ceramic membrane with addition of CuO increased to about nearly eight folds and more than three folds, respectively, compared to the original fly ash-based ceramic membrane. However, the pore size of the fly ash-based ceramic membrane with addition of CuO decreased to more than a-half of the original pore size. The optimum adsorption activity of each Cu(II), Zn(II), and Cd(II) ion was achieved at a pH of 4, 6, and 5, respectively. The adsorption kinetics of Cu(II), Zn(II), and Cd(II) ions on the fly ash-based ceramic membrane with addition of CuO followed the second-order pseudo kinetics model. Moreover, the isotherm study on the adsorption of Cu(II), Zn(II), and Cd(II) ions on the fly ash-based ceramic membrane with addition of CuO followed the Langmuir isotherm model. The adsorption capacity of the fly ash-based ceramic membrane with addition of CuO for Cu(II), Zn(II) and Cd(II) ions was 205 mmol/g, 188 mmol/g, and 111 mmol/g, respectively. This study showed clearly that the fly ash-based ceramic membrane with addition of CuO was an effective adsorbent for the adsorption of Cu(II), Zn(II) and Cd(II) ions.

© 2023 The Author(s). Published by Elsevier B.V. on behalf of King Saud University. This is an open access article under the CC BY-NC-ND license (<http://creativecommons.org/licenses/by-nc-nd/4.0/>).

## 1. Introduction

Due to industrialization and population increase, water contamination by heavy metals have been a major problem in the world. The exposure of heavy metals into human's body would be related to the human's health problems, such as mental retardation, kidneys damage, cancers, liver and lungs damage, bones fragility and even death (Jaishankar, et al., 2014). Overcoming the water

pollution due to contamination of heavy metals has been considered as a crucial effort and been paid a huge interest. Several techniques such as adsorption, electrocoagulation, chemical oxidation, ozonation, degradation, and filtration of membranes (Arellano-Cárdenas et al., 2013; Chowdhury et al., 2011) have been used to for wastewater treatment. Adsorption has been considered as one of the most effective techniques for the removal of heavy metals from wastewater due to its low-cost, simple and efficient properties (He et al., 2016; Xu et al., 2013).

Coal fly ash is a major solid waste produced from coal combustion, typically in power generation systems in Indonesia. Coal fly ash, after a modification, showed a large surface area with a porous surface and a strong adsorption capacity (Li et al., 2017). Moreover, coal fly ash is hydrophobic, environmentally friendly, and biodegradable (Dubey et al., 2015). Utilization of coal fly ash as an adsorbent for heavy metals-containing wastewater treatment could be a beneficial way to overcome the solid waste problems of coal combustion, as well as those related to the heavy metal contamination in water.

\* Corresponding author.

E-mail addresses: [fwidhi\\_kimia@mail.unnes.ac.id](mailto:fwidhi_kimia@mail.unnes.ac.id) (F.W. Mahatmanti), [jumaeri.kimia@mail.unnes.ac.id](mailto:jumaeri.kimia@mail.unnes.ac.id) (J. Jumaeri), [ella.kusuma@mail.unnes.ac.id](mailto:ella.kusuma@mail.unnes.ac.id) (E. Kusumastuti).

Peer review under responsibility of King Saud University.



Production and hosting by Elsevier

<https://doi.org/10.1016/j.jksus.2023.102866>

1018-3647/© 2023 The Author(s). Published by Elsevier B.V. on behalf of King Saud University.

This is an open access article under the CC BY-NC-ND license (<http://creativecommons.org/licenses/by-nc-nd/4.0/>).

The utilization of coal fly ash as an adsorbent for heavy metal removal has been extensively studied. However, the relatively low adsorptive capacity of the fly ash adsorbent was reported. The use of coal fly ash as an adsorbent during the adsorption of Pb(II), Ni(II) and Cr(VI) ions showed a relatively low adsorption activity, unless a modification towards the fly ash was employed (Shyam et al., 2013). Similar results were reported when coal fly ash was used as an adsorbent during the adsorption of Pb(II), Cd(II) and As(III) (Chen et al., 2023). The structure transformation of original coal fly ash to a ceramic membrane could improve the adsorption activity of the fly ash and could be due to its higher porosity and permeability resulted by the smaller pore sizes and higher flexural strength (Wang et al., 2019).

An additive often needs to be used to obtain a ceramic membrane with good characteristics, as well as good performance. The addition of 3 wt% of CuO to a hollow fibre ceramic membrane has been reported to be able to improve the maximum flexural strength of the ceramic membrane to 116.78 MPa (Wang et al., 2019). The increase in the maximum flexural strength of the ceramic membrane could promote the ability of the ceramic membrane as a catalyst (Lu et al., 2014), such as in the membrane activation (Zhang et al., 2014; Hu et al., 2017; Zhang et al., 2013). The addition of CuO to the fly ash-based ceramic membrane would also improve the flexural strength of the membrane due to the formation of hydrogen bonding between the Si-O-H chain of the ceramic membrane and  $O^{2-}$  of the added CuO (Wang et al., 2019). The synthesis of fly ash ceramic membrane with the addition of CuO as an adsorbent of heavy metals, such as Cu(II), Zn(II) and Cd(II) has not been reported before. Therefore, this study investigated the effect of the addition of CuO on the characteristics and adsorption performance of the fly ash-based ceramic membrane. The adsorption performance was examined towards individual Cu(II), Zn(II) and Cd(II) heavy metal ions under various conditions, i.e., pH, contact time and initial concentration of heavy metal ions. Moreover, the adsorption isotherm and kinetics of Cu(II), Zn(II) and Cd(II) over the fly ash-base ceramic membrane with addition of CuO were analyzed and formulated.

## 2. Materials and methods

This study used coal fly ash obtained from the O&M Business and Service Units of PT. Pembangunan Jawa Bali, Rembang, Central Java, Indonesia. Ethanol (98%, Merck) and CuO (99%, Merck) were used in the preparation of milled fly ash and CuO prior to the synthesis of CuO-modified fly ash ceramic membrane. Polyethylene glycol (PEG) 1000 and technical polyvinyl alcohol (PVA) with a molecular weight of 13,000–23,000 g/mol were used as plasticizers during the synthesis of fly ash-based ceramic membrane. Nitrate hydrate salts of Cu(II), Zn(II), and Cd(II) ions were used as the standards during the quantification of the metal ions using calibration curve method with an average  $R^2$  value  $\geq 0.95$ .

### 2.1. Preparation of milled fly ash and CuO

Coal fly ash powder was first calcined at 600 °C for 3 h and then sieved through a 147  $\mu\text{m}$  sieve. The fly ash was mixed with ethanol and milled using a HEM 3D-E ball milling machine type PM 200 Retsch for 30 min and then dried at 90 °C for 24 h (Liu et al., 2016). The same treatment was employed for the mixture of ethanol and CuO powder.

### 2.2. Synthesis and characterization of fly ash ceramic membranes

The milled fly ash was mixed with 3 wt% CuO. Meanwhile, a total of 0.3 g PEG was added to the 3.4 g PVA solution. This mixture

of PEG and PVA was added to 25 g of the mixture of milled fly ash and 3 wt% CuO. The resulting mixture was poured into a membrane mould with a diameter of 50 mm with a thickness of 2–3 mm. The resulted paste was dried at room temperature for 24 h. The wet half membrane was heated in a furnace at 1100 °C for 2 h (Wang et al., 2019). The membrane was further heated in a furnace at 1100 °C for another 2 h (Liu et al., 2016). The membrane obtained from this process was called as C3. Similar steps of synthesis were also carried out without the addition of CuO. The ceramic membrane obtained was called as C0.

Both fly ash ceramic membranes (with and without the addition of CuO) were characterized by using a FEI Quanta 650 scanning electron microscope to surface morphology of the ceramic membranes. A Shimadzu XRD-7000 X-ray diffractometer was also used to investigate the crystallinity and the phases existed in the ceramic membranes. In addition, the thermal stability and surface porosity of the synthesized ceramic membranes were analyzed using a Hitachi High-Tech STA 7300 Thermogravimetric Analyzer and Quantachrome Nova 1200e surface area analyzer.

### 2.3. Batch sorption experiments

#### 2.3.1. The effect of pH

The performance test towards the fly ash-based ceramic membranes with and without the addition of CuO as an adsorbent for Cu(II), Zn(II), and Cd(II) ions was carried out using a batch method, as reported earlier (Mahatmanti et al., 2016). Each adsorption experiment involved an individual metal ion; no mixture of metal ions was used. In each experiment, 0.10 g of the C0 or C3 ceramic membrane with the particle size of  $< 147 \mu\text{m}$  was added to 50 mL of individual Cu(II), Zn(II), and Cd(II) ion solutions with a concentration of 0.4 mmol/L at pHs of 2–8. The mixture was then shaken under a mechanical stirring of 150 rpm for 2 h. The solution was separated from the membrane through a filtration using a Whatmann No. 42 filter paper. The concentration of Cu(II), Zn(II), and Cd(II) metal ions remained in the solution was quantified by using a Perkin Elmer Analyst 400 atomic absorption spectrophotometer.

#### 2.3.2. The effect of contact time

To study the effect of the contact time during the adsorption of Cu(II), Zn(II), and Cd(II) metal ions over the fly ash-based ceramic membranes with and without the addition of CuO, the adsorption experiments were carried out with various length of time (0, 15, 30, 60, 90, 120, and 150 min). The experimental procedure was the same as that on the effect of pH, except the pH value and the length of the contact time. Typically, in each experiment, 50 mL of individual Cu(II), Zn(II), and Cd(II) ion solutions with a concentration of 0.4 mmol/L was mixed with 0.1 g of C0 or C3 fly ash ceramic membrane with a pH of the optimum pH value obtained from the previous step of experiments. All mixtures were shaken for 0, 15, 30, 60, 90, 120, and 150 min under a mechanical stirring of 150 rpm. The solution was separated from the membrane through a filtration using a Whatmann No. 42 filter paper. The concentration of Cu(II), Zn(II), and Cd(II) metal ions remained in the solution was quantified by using a Perkin Elmer Analyst 400 atomic absorption spectrophotometer.

#### 2.3.3. The effect of the initial concentration of metal ions

To study the effect of the initial concentration of the metal ions, solutions of metal ions with an initial concentration of 0.1–0.7 mmol/L were used. A 50 mL of each concentration of each metal ion was added to 0.1 g of C0 or C3 fly ash ceramic membranes at an optimum pH and shaken out during the optimum contact time (both were obtained from previous step of experiments) under a mechanical stirring of 150 rpm. The solution was separated from the membrane through a filtration using a Whatmann No. 42 filter

paper. The concentration of Cu(II), Zn(II), and Cd(II) metal ions remained in the solution was quantified by using a Perkin Elmer Analyst 400 atomic absorption spectrophotometer.

### 3. Result and discussion

#### 3.1. Ceramic membrane characteristics

Surface characteristics of ceramic membranes such as pore surface area, pore-volume, and average pore diameter of C0 and C3 were determined using BET analysis obtained from N<sub>2</sub> adsorption/desorption analysis as shown in Fig. 1. The surface area of the C3 membrane increased from 0.834 m<sup>2</sup> g<sup>-1</sup> to 6.268 m<sup>2</sup> g<sup>-1</sup>. The total pore volume increased from 1.974 × 10<sup>-3</sup> cc g<sup>-1</sup> to 6.763 × 10<sup>-3</sup> cc g<sup>-1</sup>, but the pore size decreased from 4.735 nm to 2.158 nm. The increase in the specific surface area and the total pore volume was possibly due to of the addition of CuO, which will accelerate the growth of grains on the membrane surface (Wang et al., 2019). This grain growth causes the pore size to decrease, CuO can enter the membrane pores and reduce the pore size. Specific surface area is generally considered to be the most important property that determines adsorption capacity.

The morphology analysis of ceramic membrane using Scanning Electron Microscope (SEM) was used with the 2000 times magnification. The SEM images are presented in Fig. 2.

Ceramic membrane with the CuO addition produces membrane with more spaced pores, as seen in Fig. 2 (b). The CuO addition causes the pores on the membrane surface to become covered by CuO (Lü et al., 2014; Ruan et al., 2017).

The ceramic membrane without the CuO addition showed a pore size radius that tended to be greater than the that with the CuO addition, with a smaller pore volume total on the membrane without the CuO addition. The increase in the pore volume total results from the increasing densification process on the membrane, which is indicated by the growth of granules in the membrane components from the liquid phase during the sintering process (Wang et al., 2019).

The phase and crystallinity analyses of both the raw material and ceramic membranes are depicted in Fig. 3. The diffractograms of fly ash and CuO are employed as the primary materials for synthesizing the ceramic membranes. The peaks indicating the presence of SiO<sub>2</sub> are observed as quartz at 2θ = 22, and as mullite

(3Al<sub>2</sub>O<sub>3</sub>. 2SiO<sub>2</sub>) at 2θ = 29, 35, and 40, with low intensities in the fly ash. During the membrane formation process, new mineral phases were identified, namely halite at 2θ = 32 and illite at 2θ = 41. The crystallinity of each phase increased as the addition of CuO. Additionally, characteristic peaks corresponding to monoclinic CuO are observed in the XRD spectrum of C3 at 2θ = 35.6 and 38.9 (Kanakaraju et al., 2020).

The analysis of the thermal stability of ceramic membranes is depicted in Fig. 4. It is an evident that both C0 and C3 experienced a weight loss of approximately 0.1% and 0.2%, respectively, at 120 °C. This indicates that both C0 and C3 exhibited commendable stability and minimal water content. Continuous weight losses were observed in both C0 and C3 up to 400 °C, signifying the decomposition of residual hydrocarbons used as binders during the preparation process. Intriguingly, a weight gain of approximately 0.8% and 0.5% was observed for C0 and C3, respectively. This outcome implies the formation of an oxidized state of metal in the raw material derived from fly ash (Shanholtz et al., 2017). According to Akter et al. (2021), the CuO addition can increase the thermal resistance of the membrane because CuO provides a solid attractive force among the ions on each oxide and this attractive force requires a large amount of energy to break.

#### 3.2. Adsorption properties of ceramic membrane

The ability test of the ceramic membrane as the adsorbent of metal ions in water was carried out on solutions containing Cu (II), Zn(II), and Cd(II) ions using a batch system. In the metal ion adsorption process, the influence of variables: (a) pH of metal ion solution, (b) contact time, and (c) initial concentration of metal ion, was studied.

##### 3.2.1. Effect of pH of the solution on metal ion adsorption by C0 and C3 ceramic membranes

The adsorption ability of the ceramic membrane against Cu(II), Zn(II), and Cd(II) ions is strongly influenced by the pH of the metal ion solution. This pH variation assessed the effect on the adsorption of several metal ions, which was carried out in the 2–8 range. The comparison of the adsorption of Cu(II), Zn(II), and Cd(II) ions on solution pH variation for ceramic membranes is presented in Fig. 5.

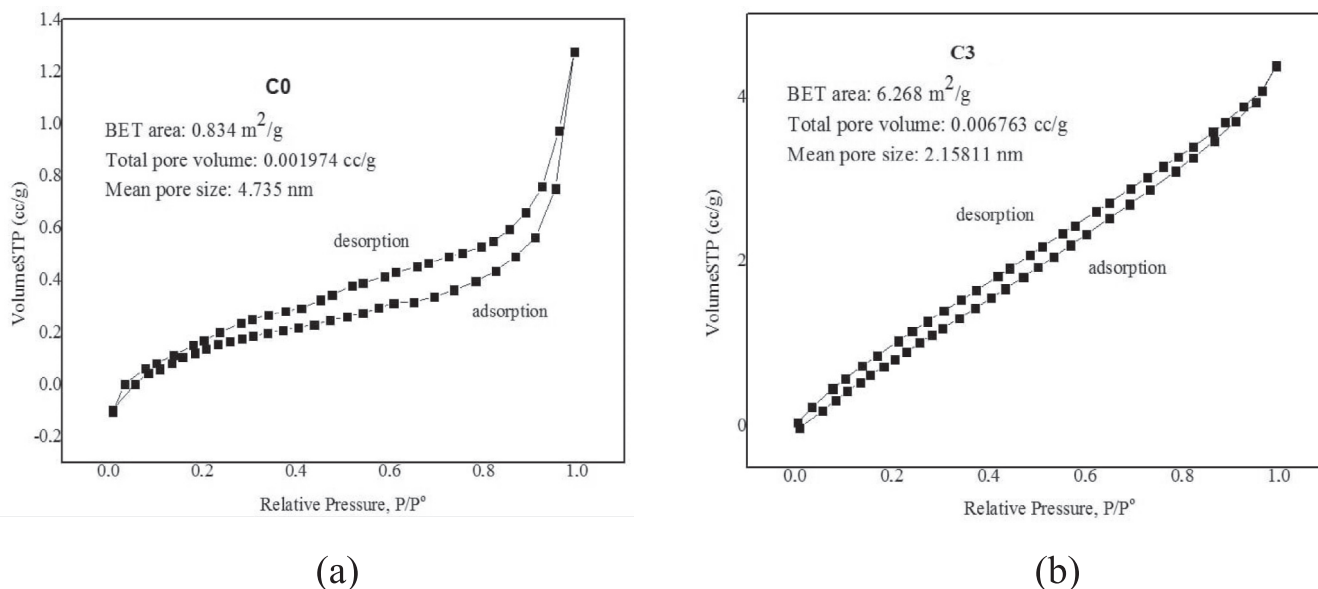


Fig. 1. BET analysis obtained from N<sub>2</sub> adsorption/desorption analysis.

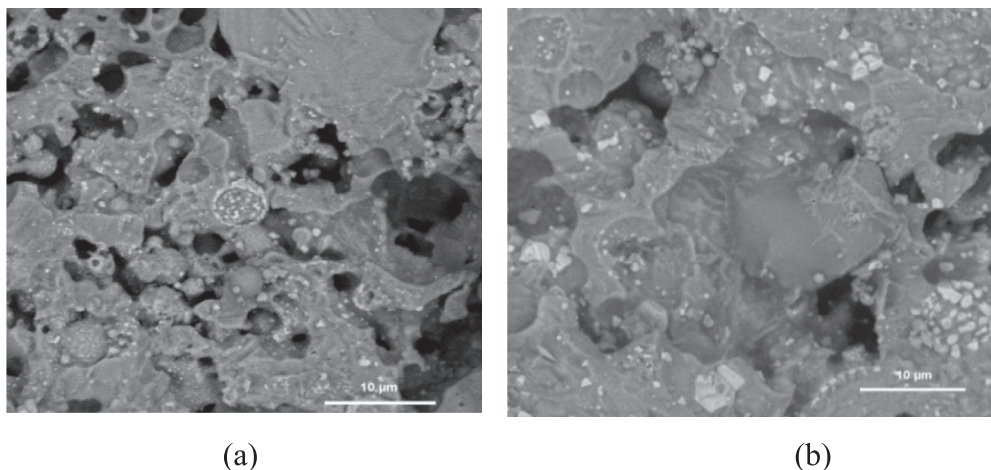


Fig. 2. Membrane SEM images with 2000 magnification, (a) C0 membrane and (b) C3 membrane.

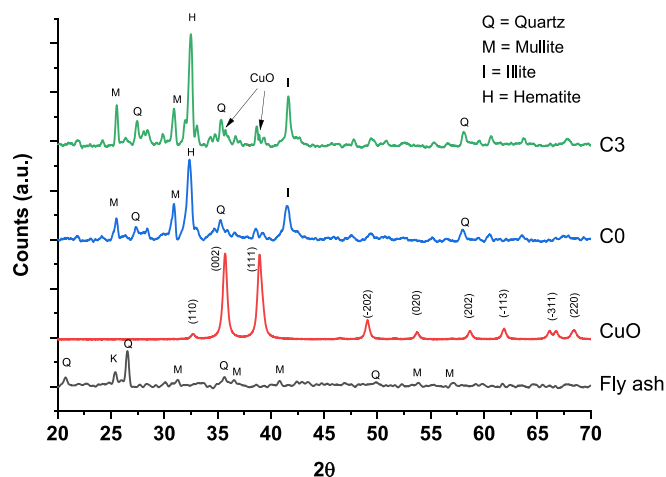


Fig. 3. The diffractograms of fly ash, CuO, C0 and C3.

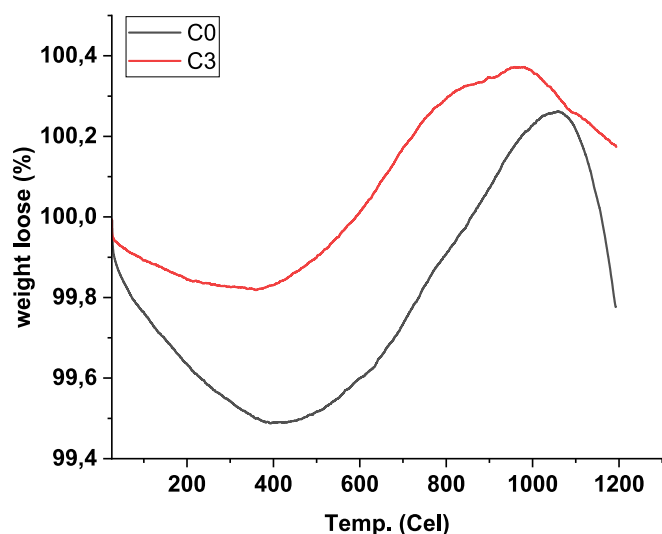
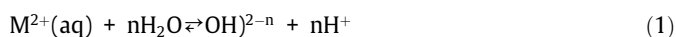


Fig. 4. TGA diffractogram on C0 and C3 ceramic membranes.

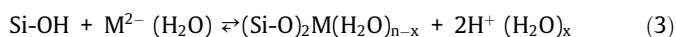
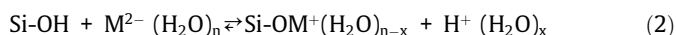
In general, it can be seen that the higher the pH of the solution, the adsorption of metal ions increased and reached the optimum condition in the pH range of 4–6. A decrease in the adsorption

was observed in the pH above 6. It can be seen concretely that the characteristics of each metal ion adsorbed on all membranes, the Cu(II) ions were optimally adsorbed at pH = 4. The Cd(II) ions were optimally adsorbed at pH 5, and Zn(II) was optimally adsorbed at pH = 6.

Assuming that the metal ions adsorption by all membranes involves the active site  $[Al(OH)_4]^-$  on the adsorbent surface, at pH 2–6 (high acidity), speciation of Cu(II), Cd(II), and Zn(II) ions occur. The absorption mechanism that occurs in the membrane was thought to be due to an electrostatic reaction between the negatively charged membrane surface and the positively charged Cu (II), Cd(II), and Zn(II) ions. At pH 7–8, Cu(II), Cd(II) and Zn(II) ions tended to precipitate. This causes a decrease in the adsorption because it is predicted that electrostatic repulsion occurred between the membrane surface and metal ions which are both negatively charged. According to Visa (2016), the mechanism of the metal ion adsorption process on ceramic membranes can be explained by reaction (1), namely the formation of metal ions which are hydrolyzed into their hydrates:



Cu(II), Cd(II), and Zn(II) ions can also be adsorbed through the silanol (Si-OH) group that is on the surface of the adsorbent (Visa and Chelaru, 2014) as written in the reactions (2) and (3).



### 3.2.2. The effect of contact time on the adsorption of metal ions by ceramic membranes

In this study, the kinetics parameters were obtained by interacting with each metal ion at the optimum pH and room temperature, as well as the time variation from 15 to 150 min. The observation results of the contact time effect on each metal ion are presented in Fig. 6. At the contact time between 15 and 150 min, there was an increase in the number of adsorbed metal ions. This indicates that there had been an equilibrium between the number of metal ions adsorbed and the number of ions the metal ions remaining in solution. Referring to Fig. 6, the adsorption data at various contact times can be processed using the first pseudo-order kinetics model, which is proposed by Lagergren, and the second pseudo-order kinetics model, which Ho proposes. Several previous researchers used Lagergren's first pseudo-order kinetics equation and the second pseudo-order kinetics (Ho) to

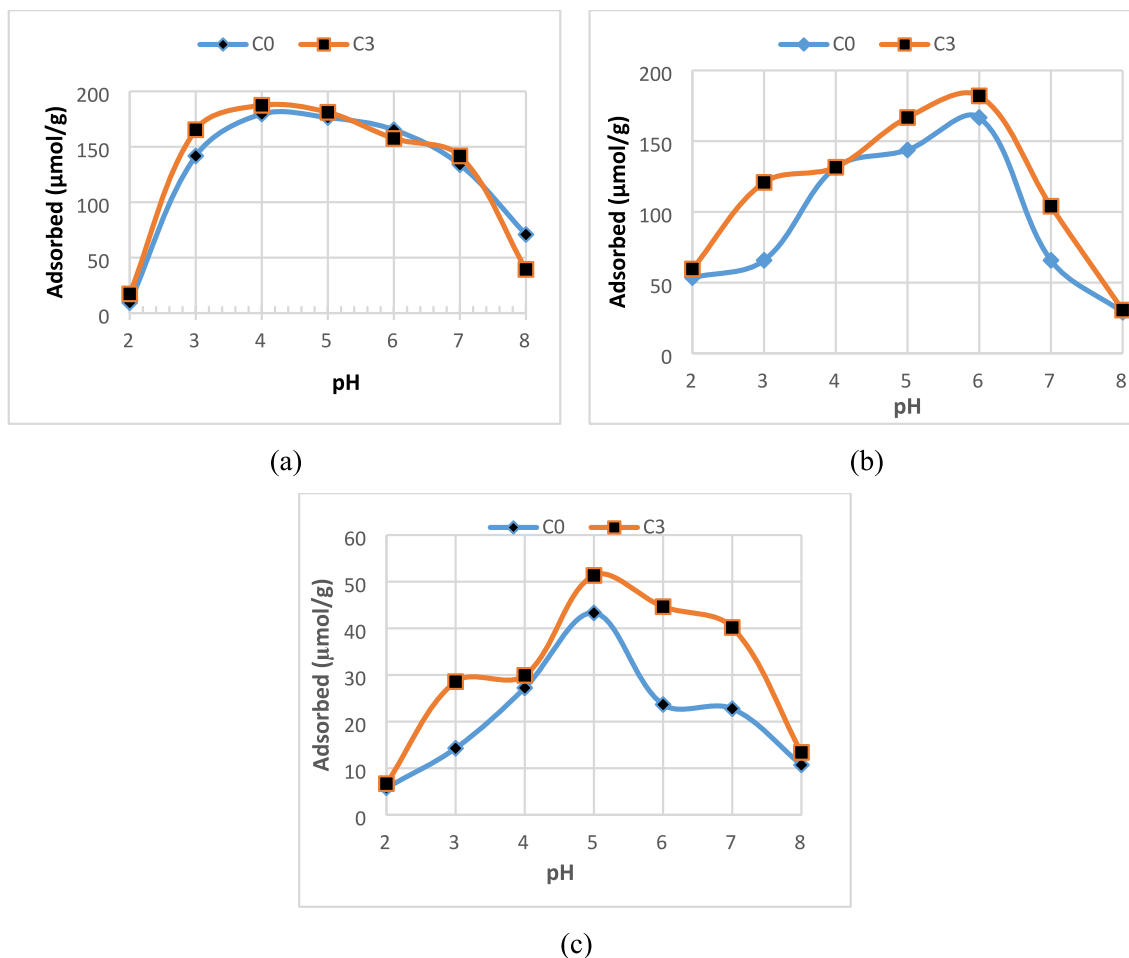


Fig. 5. The comparison of the adsorption of (a). Cu(II), (b). Zn(II), and (c). Cd(II) metal ions at the pH variation of the solutions under condition of initial concentration 0.4 mmol/L, stirring 150 rpm, and contact time 2 h.

evaluate the trend of the kinetics model that applies to the metal ion adsorption process by the adsorbents made from fly ash (Chaudhary et al., 2013; Foorginezhad and Zerifat, 2017; Hubadillah et al., 2017).

Lagergren’s first pseudo-order kinetics equation:

$$\log(q_e - q_t) = \log q_e - (k_1/2,303) t \tag{4}$$

Note:  $q_e$  = the amount of adsorbate at the equilibrium (mmol  $g^{-1}$ ),  $q_t$  = the amount of adsorbate at t time (mmol  $g^{-1}$ ), t = time (minutes),  $k_1$  = the first pseudo - order constant rate (minute $^{-1}$ ).

The second pseudo- order kinetic equation (Ho):

$$\frac{1}{q_e - q_t} = \frac{1}{q_e} + k_2 t \tag{5}$$

Note:  $q_e$  is the amount of adsorbate at the equilibrium (mmol  $g^{-1}$ ),  $q_t$  is the amount of adsorbate at t time (mmol  $g^{-1}$ ), t is the time in minutes and  $k_2$  is the second pseudo order constant rate (g mmol $^{-1}$  min $^{-1}$ ). The data processing results that use Lagergren’s first pseudo-order kinetics equation and the second pseudo-order kinetics (Ho) equations are presented in Table 1.

The  $R^2$  coefficient of determination value data presented in Table 1 provided some significant data between the results obtained through Lagergren’s first pseudo-order kinetics model and the second pseudo-order kinetics model. In general, there was a tendency for the  $R^2$  coefficient of determination value to be higher in the second pseudo-order kinetics model.

Based on the  $k_2$  value in Table 1, it was found that the  $k_2$  of Cu(II) ion has the lowest value compared to that of other ions on the C0 and C3 membranes, the velocity of Cu(II) ions is slower than other ions. The adsorption is possible through the pores on the membrane surface so that the ion which has a larger size (radius) will be absorbed more slowly. The data for the anhydrate radius and the hydrated radius are presented in Table 2.

Based on the data for the anhydrate radius and the hydrated radius in Table 2, the rate of ions reaction should be Cu(II) > Cd(I I) > Zn(II). The addition of CuO in the manufacture of ceramic membranes causes most of the membrane surface to be covered by CuO. This would reduce the diffusion rate of metal ions due to smaller pores size on the membrane.

### 3.2.3. The effect of initial metal ion concentration on metal ion adsorption by ceramic membranes

Thermodynamic studies were carried out to determine the type of membrane adsorption isotherm against metal ions. Fig. 7 shows the effects of metal ion initial concentration on adsorption of each metal ion in all membranes. The observation results on all metal ions and all membranes show an increase in the number of metal ions adsorbed and the increase in metal ion concentration. At the higher concentrations, the increase in metal ion concentration was not accompanied by a significant increase in metal ion adsorption. Evaluation of the adsorption data using the Langmuir isotherm model and the Freundlich isotherm model was carried out by transforming the adsorption data into variables according to

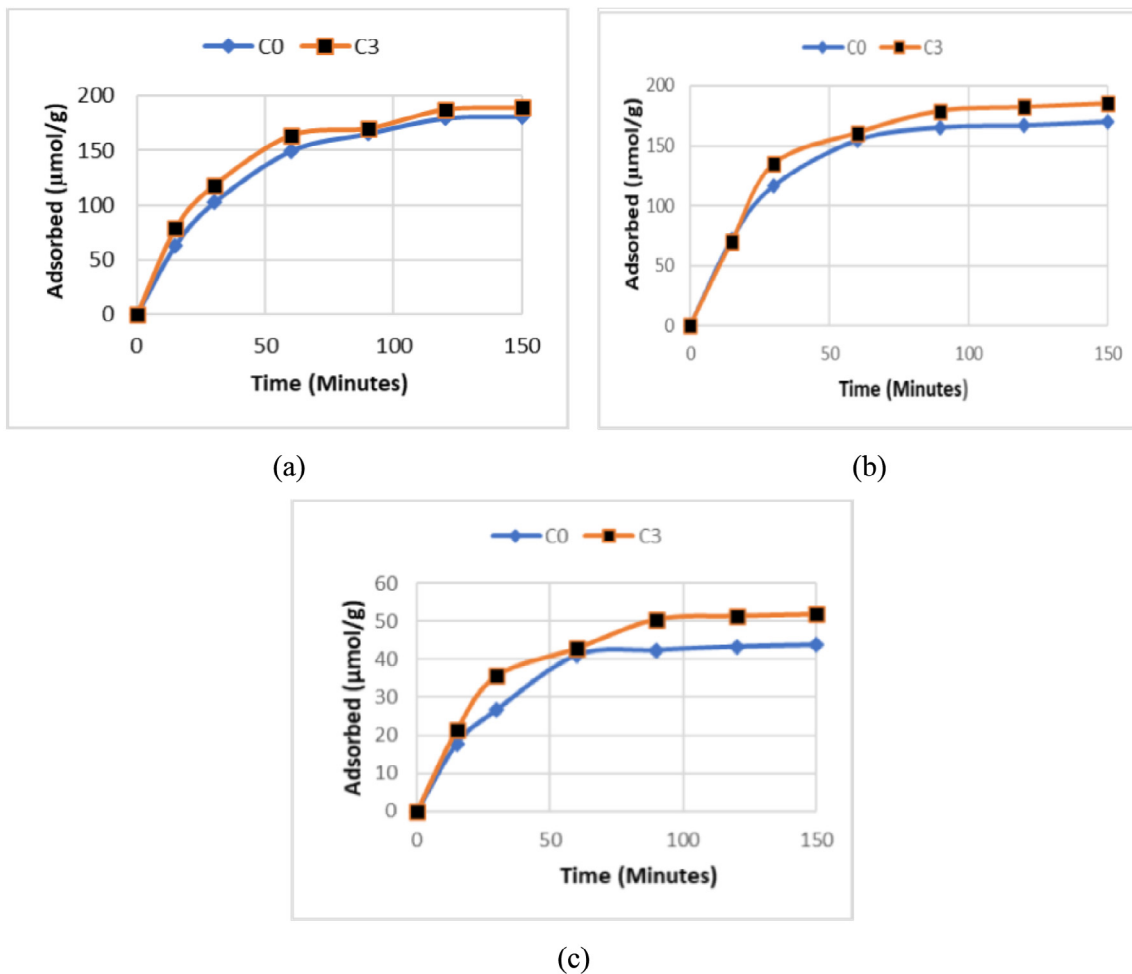


**Fig. 6.** The comparison of the adsorption of (a) Cu(II), (b) Zn(II), and (c) Cd(II) metal ions at the variation of contact time under condition of initial concentration 0.4 mmol/L, stirring 150 rpm, and the working pH of 4, 5, and 6 for Cu(II), Cd(II), and Zn(II), respectively.

**Table 1**  
Kinetics parameters of the first pseudo-order and the second pseudo-order kinetics models on the metal ion adsorption process by the ceramic membrane.

Ion	MembraneCode	Lagergren's first pseudo-order kinetics model			The second pseudo-order kinetics model		
		$k_1(\text{min}^{-1})$	$q_e(\mu\text{mol/g})$	$R^2$	$k_2(\text{g}/\mu\text{mol min}^{-1})$	$q_e(\mu\text{mol/g})$	$R^2$
Cu (II)	C0	0.0091	2.6028	0.814	0.00187	14.62	0.9960
	C3	0.0074	2.1966	0.800	0.00268	14.25	0.9974
Zn (II)	C0	0.0071	2.0579	0.722	0.09195	11.27	0.9927
	C3	0.0075	2.1583	0.672	0.00293	14.29	0.9915
Cd (II)	C0	0.0079	2.210	0.754	0.00685	5.866	0.9901
	C3	0.0073	2.131	0.765	0.01774	16.21	0.9998

**Table 2**  
Properties of metal ions (Visa, 2016).

Metal Ion	The radius of anhydrate ion (nm)	The radius of hydrated ion (nm)	Hydrolysis Constant (log $K_h$ )	Electronegativity
Cu(II)	0.072	0.295	8.00	1.95
Zn(II)	0.074	0.430	8.96	1.65
Cd(II)	0.097	0.426	10.80	1.69

the Langmuir and Freundlich isotherm linear equation models. Langmuir and Freundlich's isotherm parameter data are presented in Table 3.

The phenomena that occurred in the interaction of Cu(II), Zn(II), and Cd(II) metal ions with the active site on the membrane follow the Langmuir isotherm model. The Langmuir isotherm concept sta-

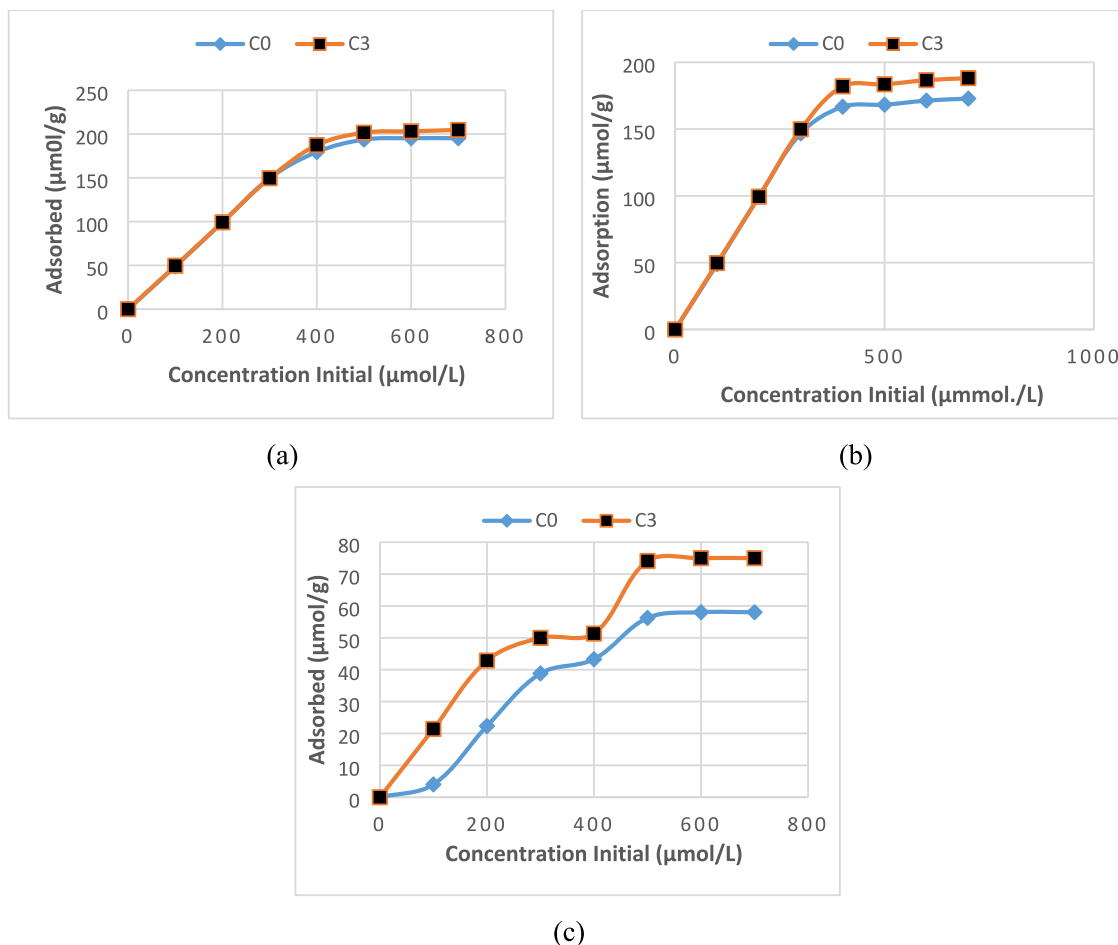


Fig. 7. The comparison of the adsorption of (a) Cu(II), b) Zn (II), and (c) Cd(II) metal ions at the variation of the initial concentration of metal ions (0.1 – 0.7 mmol/L) under condition, stirring 150 rpm, contact time 2 h and the working pH of 4, 5, and 6 for Cu(II), Cd(II), and Zn(II), respectively.

Table 3  
Langmuir and Freundlich isotherm parameters.

Ion	Membrane Code	Langmuir Isotherm			Freundlich Isotherm		
		qe (µmol/g)	ΔG (KJ/mol)	R <sup>2</sup>	K <sub>F</sub>	n <sub>F</sub>	R <sup>2</sup>
Cu (II)	C0	197.591	31.6669	0.9997	10.961	21.231	0.9840
	C3	205.320	33.5539	0.9999	11.338	18.248	0.9752
Zn (II)	C0	173.219	32.4149	0.9998	9.049	11.641	0.8400
	C3	187.902	34.2875	0.9999	11.279	32.058	0.9748
Cd (II)	C0	87.130	20.4313	0.9450	0.266	1.216	0.9216
	C3	110.780	20.4731	0.9711	1.005	1.856	0.9738

ted that an increase follows an increase in concentration in the amount of substance adsorbed to reach an equilibrium amount. Langmuir’s adsorption theory suggested that on the adsorbent surface, there are a certain number of active sites proportional to the adsorbent’s surface area. When the active site is not saturated with adsorbate, there will be an increase in adsorption. If the adsorbate saturates the active site of the adsorbent, increasing the adsorbate concentration does not increase the amount of adsorbate adsorbed (Huang et al., 2020). The Langmuir equation indicates that the adsorption reaction mechanism occurs chemically through the occurrence of electrostatic bonds, which results in monolayer adsorption on the heterogeneous substrate. According to Visa (2016), the reaction mechanism for metal ion adsorption can be

explained by the formation of complex compounds between the active sites of silica (Si-O) and alumina (Al-O) with metal ions as shown in the reaction Eqs. (6) and (7).



Based on the data in Table 2, Cu(II) ions have the highest electronegativity value with the lowest constant value compared to Zn(II) and Cd(II) ions. The low value of the hydrolysis constant indicates that metal ions are easy to be formed into their hydrate complex. The hydrating complex of the ion will be more easily adsorbed than in the free ion form (M(II)). The possible adsorption

reaction mechanism is that metal ions are formed into their hydrate complexes which are then absorbed through pores on the membrane or through the formation of electrostatic bonds on the membrane surface (Visa, 2016). The addition of CuO to the synthesis of ceramic membranes did not significantly increase the adsorption capacity. This is probably due to a decrease in the pore size of the membrane, which was covered by the presence of CuO so that the metal ions absorbed in the membrane do not experience significant changes.

#### 4. Conclusion

The coal fly-based ash ceramic membrane with the 3% CuO addition was successfully synthesized. The addition of 3% CuO increased the surface area from 0.834 m<sup>2</sup>/g to 6.268 m<sup>2</sup>/g, the total pore volume increased from 1.974 × 10<sup>-3</sup> cc/g to 6.763 × 10<sup>-3</sup> cc/g, but the pore size decreased from 4.735 nm to 2.015811 nm. The ceramic membrane performance test as adsorbent for Cu(II), Cd(II), and Zn(II) ions using batch system found that the optimum pH = 6 for Zn(II) ions, pH = 5 for Cd(II) ions, and pH = 4 for Cu(II) ions. There was a tendency for higher R<sup>2</sup> coefficient of determination values in the second pseudo-order kinetics model for the adsorption kinetics of Cu(II), Cd(II), and Zn(II) ions on ceramic membranes in general. The adsorption isotherm of Cu(II), Zn(II), and Cd(II) ions on the ceramic membrane follows the Langmuir isotherm model. The adsorption capacity values for Cu(II), Zn(II), and Cd(II) ions are 205 mmol/g, 188 mmol/g, and 111 mmol/g, respectively.

#### Declaration of Competing Interest

The authors declare that they have no known competing financial interests or personal relationships that could have appeared to influence the work reported in this paper.

#### Acknowledgments

The authors thank Research and Community Service Institute Universitas Negeri Semarang for the research funding with number 121.23.4/UN37/PPK.3.1/2020, April 23, 2020. In addition, the authors are grateful for the kind help from Ms. Widya Aprilianti and Ms. Arum Mawar Wati during the experiments and data analysis.

#### References

Akter, J., Sapkota, K.P., Hanif, M.A., Islam, M.A., Abbas, H.G., Hahn, J.R., 2021. Kinetically controlled selective synthesis of Cu<sub>2</sub>O and CuO nanoparticles

- toward enhanced degradation of methylene blue using ultraviolet and sun light. *Mater Sci Semicond Process* 123, <https://doi.org/10.1016/j.mssp.2020.105570> 105570.
- Arellano-Cárdenas, S., López-Cortez, S., Cornejo-Mazón, M., Mares-Gutiérrez, J.C., 2013. Study of malachite green adsorption by organically modified clay using a batch method. *Appl Surf Sci* 280, 74–78. <https://doi.org/10.1016/j.apsusc.2013.04.097>.
- Chaudhary, G.R., Saharan, P., Mehta, S.K., Mor, S., Umar, A., 2013. Fast and Efficient Removal of Hazardous Congo Red from Its Aqueous Solution Using  $\gamma$ -Fe<sub>2</sub>O<sub>3</sub> Nanoparticles. *Journal of Nanoengineering and Nanomanufacturing* 3, 142–146. <https://doi.org/10.1166/jnan.2013.1120>.
- Chowdhury, S., Mishra, R., Saha, P., Kushwaha, P., 2011. Adsorption thermodynamics, kinetics and isosteric heat of adsorption of malachite green onto chemically modified rice husk. *Desalination* 265, 159–168. <https://doi.org/10.1016/j.desal.2010.07.047>.
- Dubey, S., Uma, Sujarittanonta, L., Sharma, Y.C., 2015. Application of fly ash for adsorptive removal of malachite green from aqueous solutions. *Desalination Water Treat* 53, 91–98. <https://doi.org/10.1080/19443994.2013.846552>.
- Foorginezhad, S., Zerafat, M.M., 2017. Microfiltration of cationic dyes using nanoclay membranes. *Ceram Int* 43, 15146–15159. <https://doi.org/10.1016/j.ceramint.2017.08.045>.
- He, K., Chen, Y., Tang, Z., Hu, Y., 2016. Removal of heavy metal ions from aqueous solution by zeolite synthesized from fly ash. *Environ. Sci. Pollut. Res.* 23, 2778–2788. <https://doi.org/10.1007/s11356-015-5422-6>.
- Hubadillah, S.K., Othman, M.H.D., Harun, Z., Ismail, A.F., Rahman, M.A., Jaafar, J., 2017. A novel green ceramic hollow fiber membrane (CHFM) derived from rice husk ash as combined adsorbent-separator for efficient heavy metals removal. *Ceram Int* 43, 4716–4720. <https://doi.org/10.1016/j.ceramint.2016.12.122>.
- Kanakaraju, D., bin Ya, M.H., Lim, Y.C., Pace, A., 2020. Combined Adsorption/Photocatalytic dye removal by copper-titania-fly ash composite. *Surf. Interfaces* 19, <https://doi.org/10.1016/j.surfin.2020.100534> 100534.
- Liu, J., Dong, Y., Dong, X., Hampshire, S., Zhu, L., Zhu, Z., Li, L., 2016. Feasible recycling of industrial waste coal fly ash for preparation of anorthite-cordierite based porous ceramic membrane supports with addition of dolomite. *J Eur Ceram Soc* 36, 1059–1071. <https://doi.org/10.1016/j.jeurceramsoc.2015.11.012>.
- Lü, Q., Dong, X., Zhu, Z., Dong, Y., 2014. Effect of CuO doping on sinterability, mechanical and electrical properties of Sm-doped CeO<sub>2</sub> ceramic thick membrane solid electrolytes. *Ceram Int* 40, 15545–15550. <https://doi.org/10.1016/j.ceramint.2014.07.030>.
- Mahatmanti, F.W., Nuryono, N., 2016. Adsorption of Ca(II), Mg(II), Zn(II), and Cd(II) on Chitosan Membrane Blended with Rice Hull Ash Silica and Polyethylene Glycol F. *Indonesian Journal of Chemistry* 16, 45–52.
- Ruan, S., Liu, J., Yang, E.-H., Unluer, C., 2017. Performance and Microstructure of Calcined Dolomite and Reactive Magnesia-Based Concrete Samples. *J. Mater. Civ. Eng.* 29, 04017236. [https://doi.org/10.1061/\(asce\)jmt.1943-5533.0002103](https://doi.org/10.1061/(asce)jmt.1943-5533.0002103).
- Shanholtz, E.R., LaSalvia, J.C., Behler, K.D., Walck, S.D., Giri, A., Kuwielkar, K., 2017. Chemical Interactions in B4C/WC Powder Mixtures Heated Under Inert and Oxidizing Atmospheres, Advances in Ceramic Armor, Bioceramics, and Porous Materials. *Ceram. Eng. Sci. Proc.*, 57–64 <https://doi.org/10.1002/9781119321682.ch7>.
- Visa, M., 2016. Synthesis and characterization of new zeolite materials obtained from fly ash for heavy metals removal in advanced wastewater treatment. *Powder Technol* 294, 338–347. <https://doi.org/10.1016/j.powtec.2016.02.019>.
- Visa, M., Chelaru, A.-M., 2014. Hydrothermally modified fly ash for heavy metals and dyes removal in advanced wastewater treatment. *Appl Surf Sci* 303, 14–22. <https://doi.org/10.1016/j.apsusc.2014.02.025>.
- Wang, S., Tian, J., Wang, Q., Zhao, Z., Cui, F., Li, G., 2019. Low-temperature sintered high-strength CuO doped ceramic hollow fiber membrane: Preparation, characterization and catalytic activity. *J Memb Sci* 570–571, 333–342. <https://doi.org/10.1016/j.memsci.2018.10.078>.
- Xu, X., Cao, X., Zhao, L., Wang, H., Yu, H., Gao, B., 2013. Removal of Cu, Zn, and Cd from aqueous solutions by the dairy manure-derived biochar. *Environ. Sci. Pollut. Res.* 20, 358–368. <https://doi.org/10.1007/s11356-012-0873-5>.